## Electronic Supplementary Information (ESI)

# Ambient Stable Solution-Processed Organic Field Effect Transistors from Electron Deficient Planar Aromatics: Effect of End-groups on Ambient Stability

Indrajit Giri,[a] Sagar Biswas,[a] Shant Chhetri,[a] Anwesha Choudhuri,[b] Indrajit Mondal,[c] Satyaprasad P. Senanayak,[c] Parameswar Krishnan Iyer,[b*] Debangshu Chaudhuri,[a] Ratheesh K. Vijayaraghavan[a*]

[a] *Department of Chemical Sciences, Indian Institute of Science Education and Research Kolkata, Mohanpur, Nadia, West Bengal, India-741246.*

[b] *Centre for Nanotechnology, Inian Institute of Technology Guwahati, Assam, India-781039.*

[c] Nanoelectronics and Device Physics Lab, School of Physical Sciences, National Institute of Science Education and Research, OCC of HBNI, Odisha, India-752050.

Email: pki@iitg.ac.in, ratheesh@iiserkol.ac.in

| | Table of Contents | Page No |
|---|---|---|

## 1. Characterization data:

### NMR data:

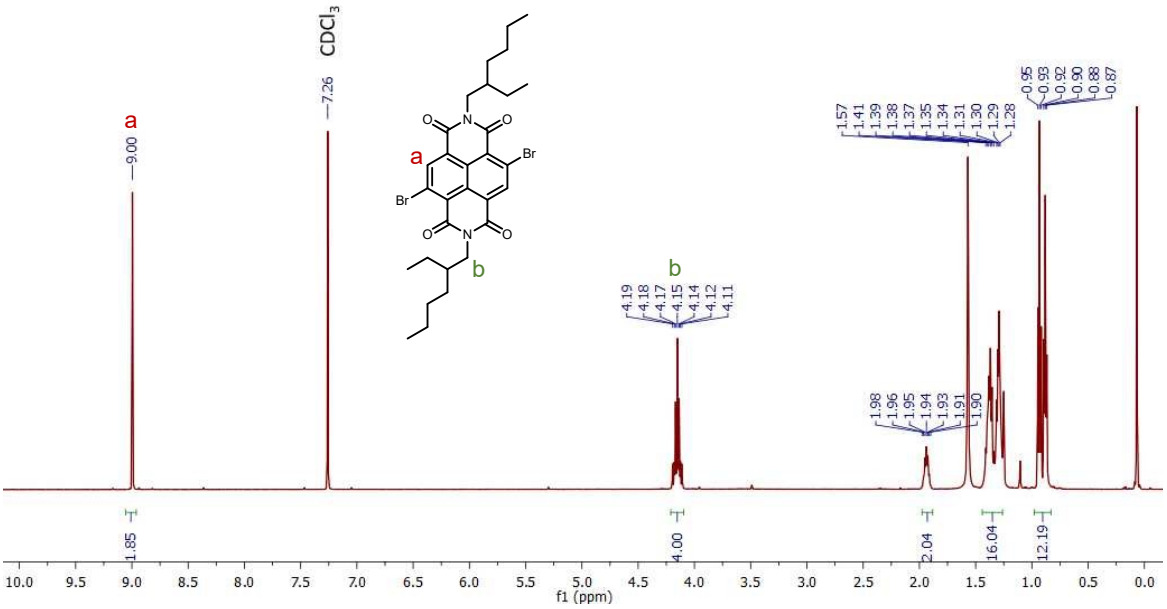


**Figure S1.** $^{1}$H NMR spectrum of **EHNDIBr$_2$** in $CDCl_3$.

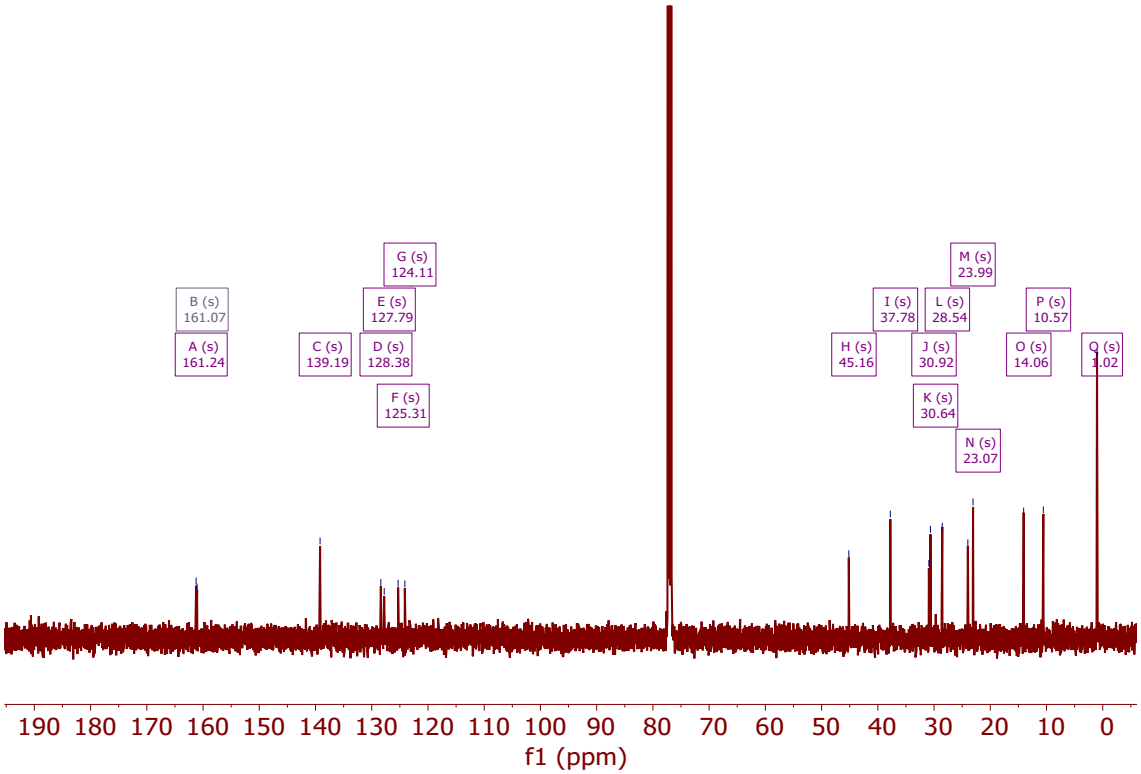


**Figure S2.** $^{13}$C NMR spectrum of **EHNDIBr$_2$** in $CDCl_3$.

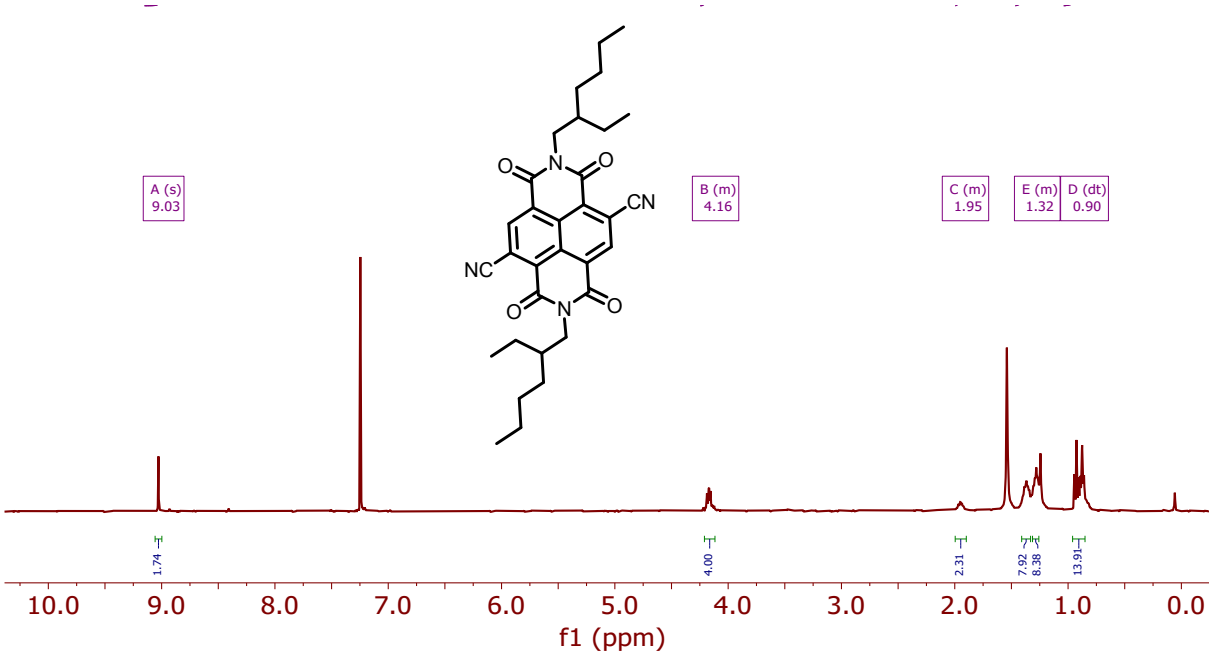


**Figure S3.** $^{1}$H NMR spectrum of **EHNDICN$_2$** in $CDCl_3$.

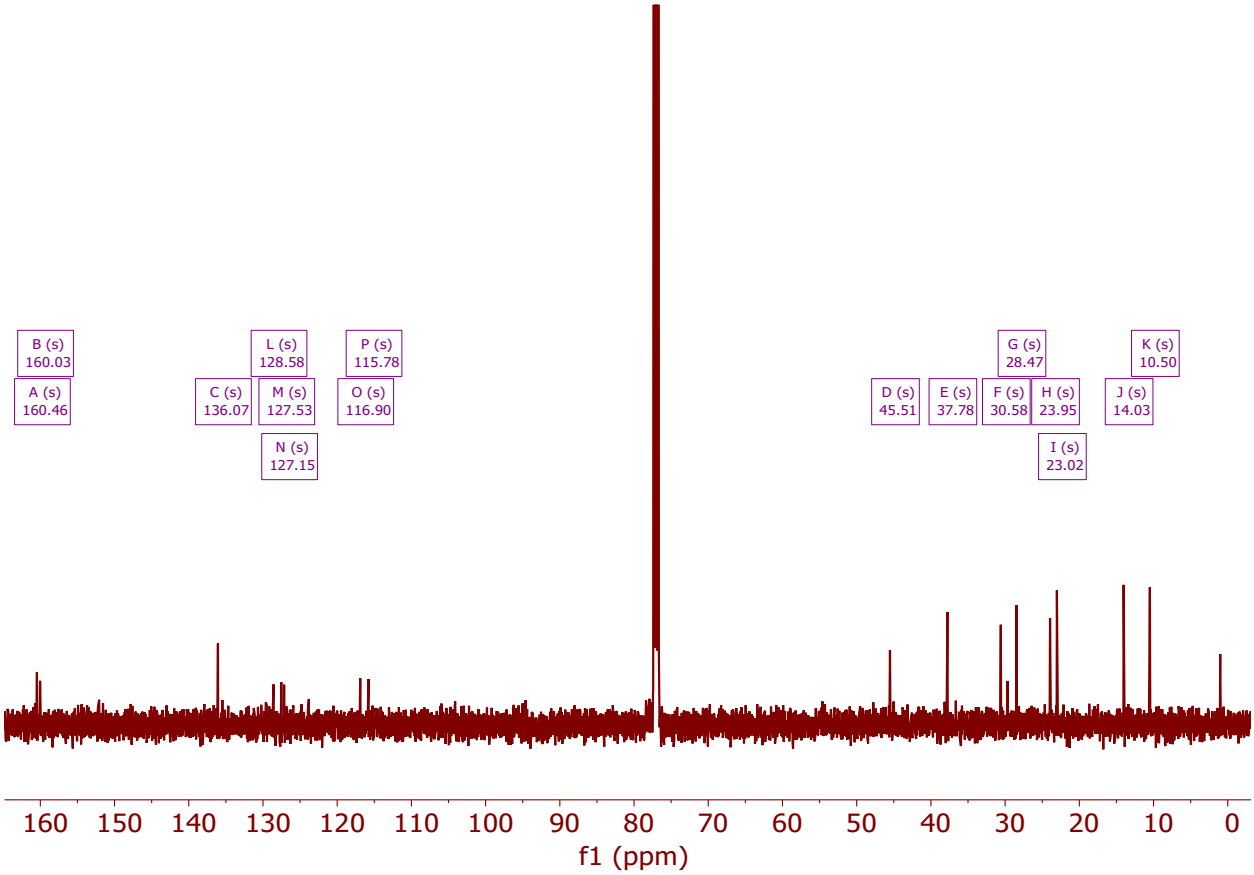


**Figure S4.** $^{13}$C NMR spectrum of **EHNDICN$_2$** in $CDCl_3$.

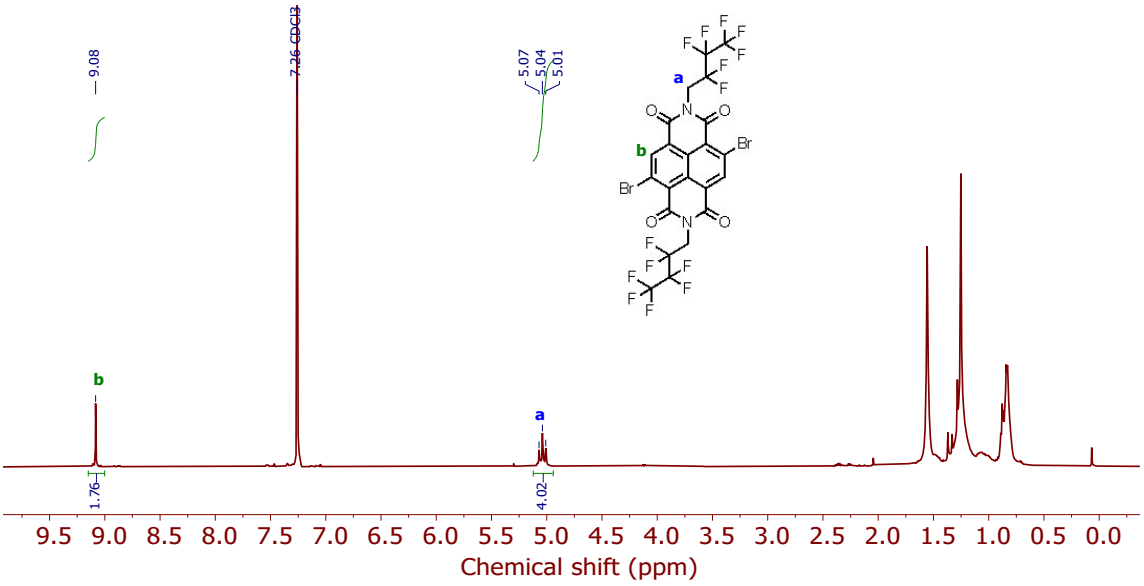


**Figure S5.** $^{1}$H NMR spectrum of **NDIFBr$_2$** in $CDCl_3$.

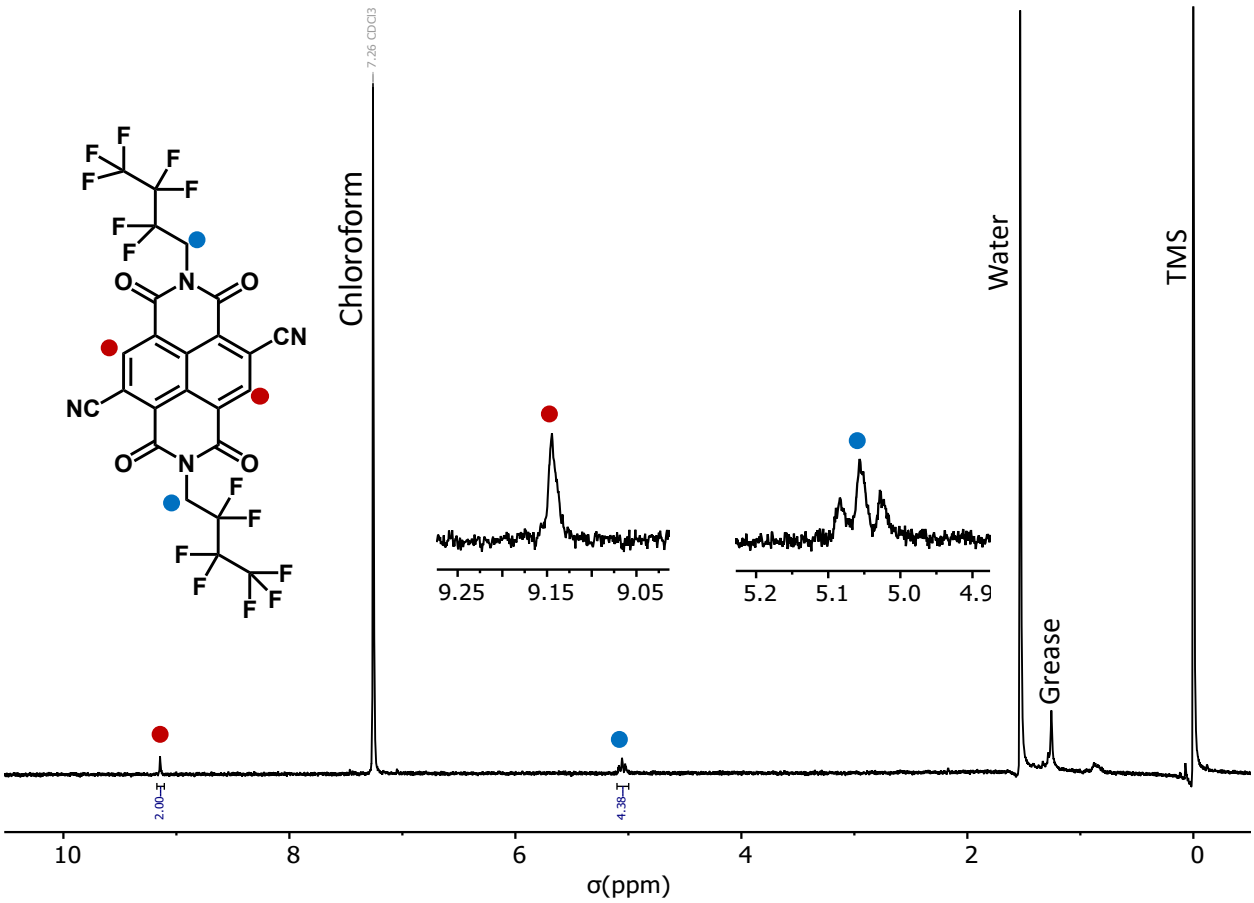


**Figure S6.** $^{1}$H NMR spectrum of **NDIFCN$_2$** in $CDCl_3$.

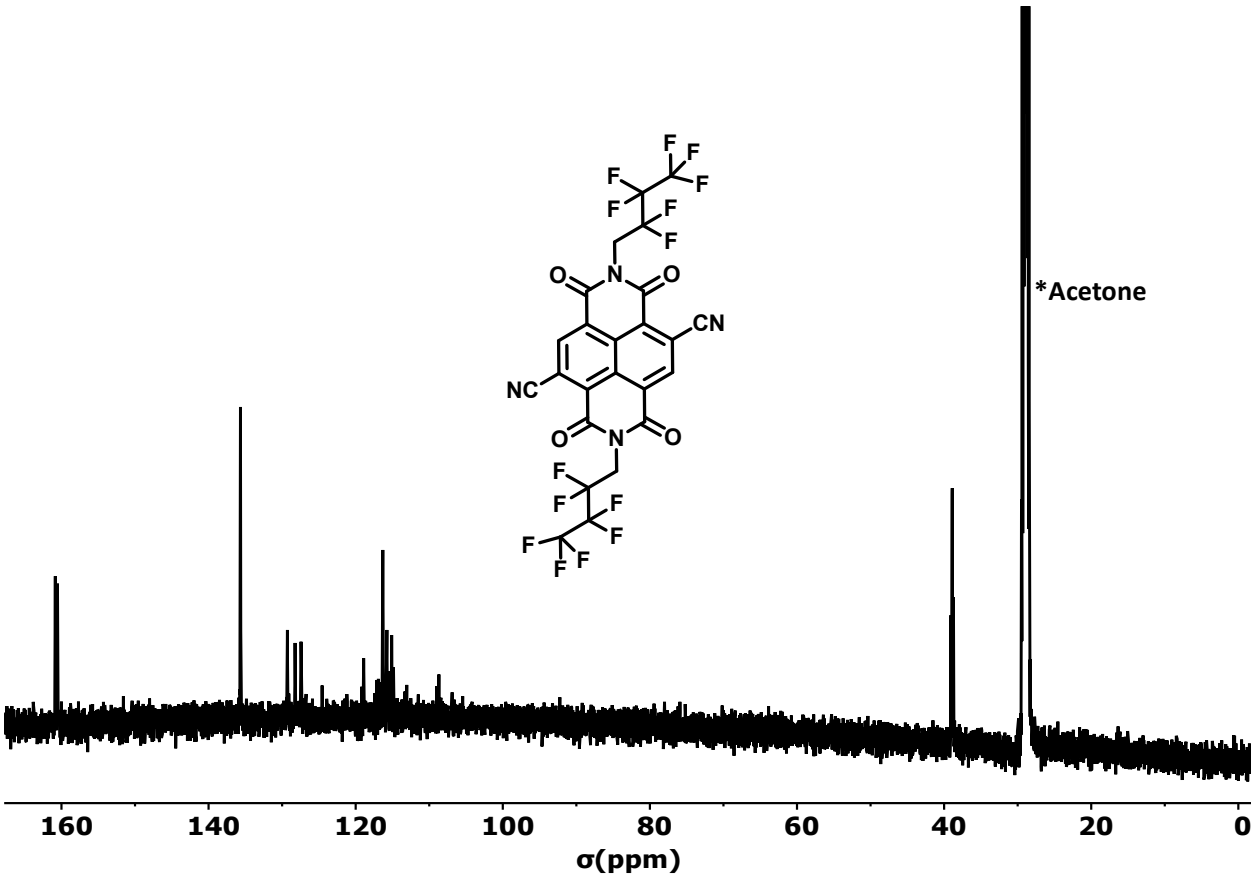


**Figure S7.** $^{13}C$ NMR spectrum of **EHNDICN$_2$** in $CDCl_3$.

## 2. Computational calculations:

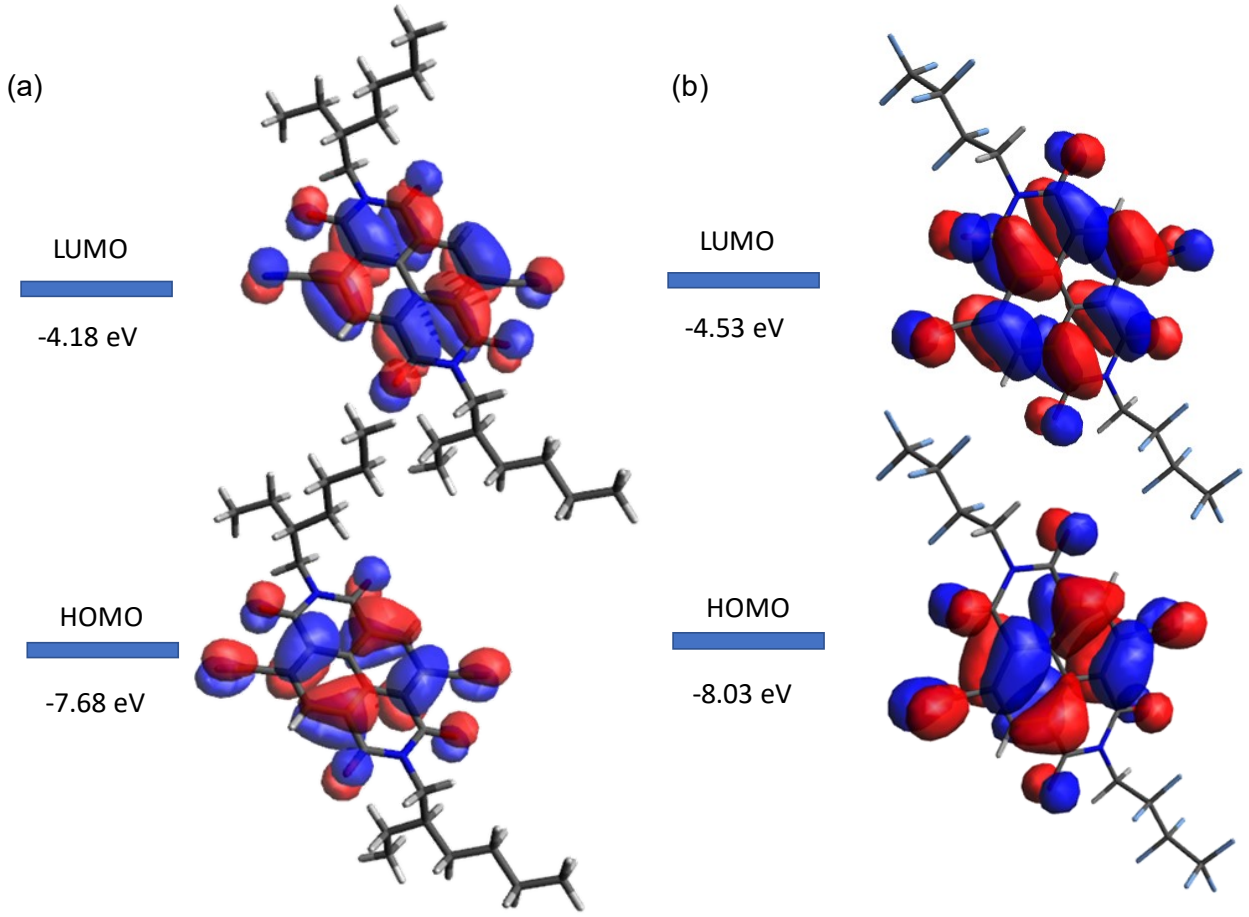


**Figure S8.** HOMO and LUMO levels and the orbital distribution diagram from DFT calculation: (a) **EHNDICN$_2$** and (b) **NDICN$_2$**.

## 3. Cyclic voltammetry (CV):

CV was carried out with the CHI604D instrument. CV for liquid state samples was determined at room temperature using 0.1 M tetrabutylammonium hexafluorophosphate ($TBAPF_6$) in dry $CH_2Cl_2$ solvent under nitrogen atmosphere with a scan rate of 100 mV/s, where gold wire used as the working electrode; platinum wire as the counter electrode; Ag/AgCl (saturated KCl) as the reference electrode. LUMO energy levels of the compounds were calculated according to the inner reference ferrocene redox couple versus $Ag/Ag^+$ in $CH_2Cl_2$ by using the formula $E_{LUMO} = -[E_{red}^{onset} + 4.8 - E^{1/2}_{Fc}]$.

## 4. Substrates wettability test:

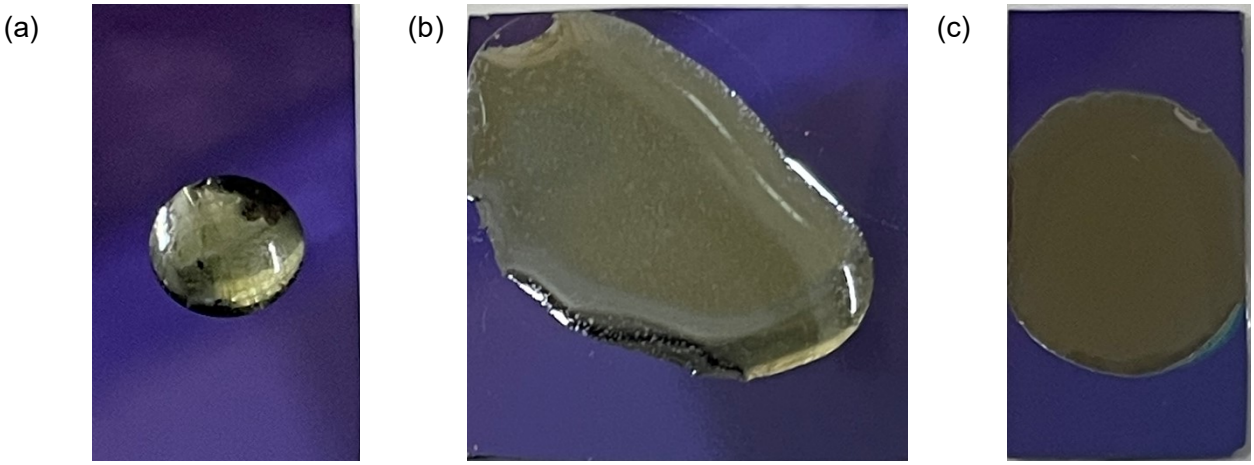


**Figure S9.** Substrate wettability: a drop solution of **$NDIFCN_2$** in *o*-DCB on (a) *n*-OTS treated $Si/SiO_2$, (b) Bare $Si/SiO_2$. (c) **$EHNDICN_2$** in $CHCl_3$ on *n*-OTS treated $Si/SiO_2$.

## 5. Device fabrication procedure (thermal vapor deposited) active layer:

For **$EHNDICN_2$**, a bottom gate top contact geometry was used. The glass substrates were cleaned by dipping the substrates in piranha solution for 1 hour followed by rinsing in DI water and drying. 100 nm of aluminum was thermally deposited on the cleaned glass substrates to form the gate electrode of width 1 mm by shadow masking on a glass substrate. A solution of PVA in DI water (100 mg $ml^{-1}$) was prepared and spin-coated with 1000 rpm for 30 s on the gate deposited substrate and dried at 100 °C for 1 hour to form 1 µm thick layer. PVA acts as the first dielectric, over which a 100 nm (3000 rpm 30 s) thick second dielectric layer (PMMA) is coated and dried at 100 °C for 1 hour. After the deposition of gate dielectric layers, a 60 nm (±10 nm) active material **$EHNDICN_2$** was deposited by thermal deposition at a temperature of 250 °C under a base pressure of $10^{-6}$ mbar at substrate temperature of 60 °C. Further, Al source–drain electrodes were thermally deposited using shadow masking to form a channel of length (L) 40 µm and width (W) 0.8 mm.

For **NDIFCN$_2$**, a bottom contact top gate geometry was used. To extract the optimized charge transport properties, we also fabricated FETs for the same molecules using a vapor deposition technique. The semiconducting films were grown on lithographically patterned 25 nm thick Cr/Au S-D electrode. This was followed by vapor-deposition of the thin films of **NDIFCN$_2$** at $10^{-6}$ Torr, at a rate of 0.2 Å/s to achieve film thickness of up to 40 nm. The temperature of the substrate was set at room temperature during the process of deposition. All the measurements were performed using a semiconductor parameter analyzer B1500.

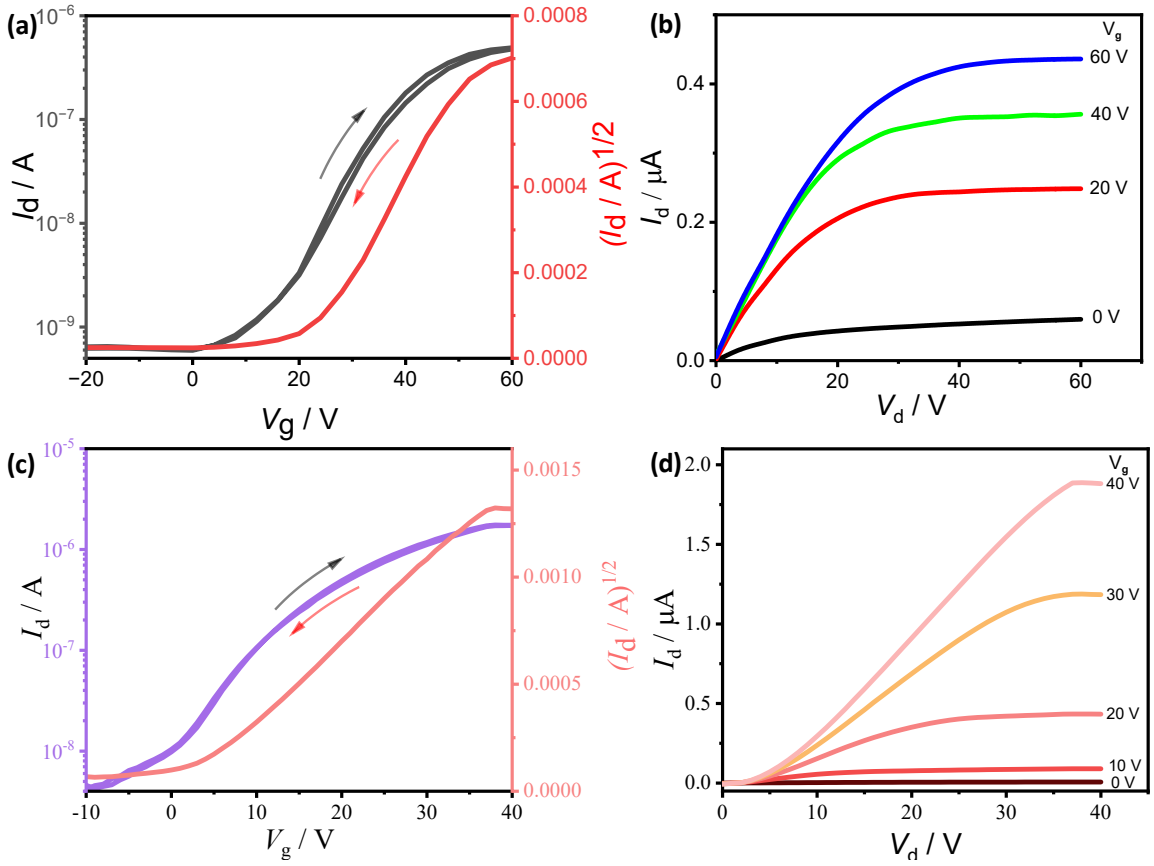


**Figure S10.** Transfer curves (a) & (c) and output curves (b) & (d) for **NDIFCN$_2$** & **EHNDICN$_2$** respectively for the devices made of Physical Vapor Deposition (PVD) method.

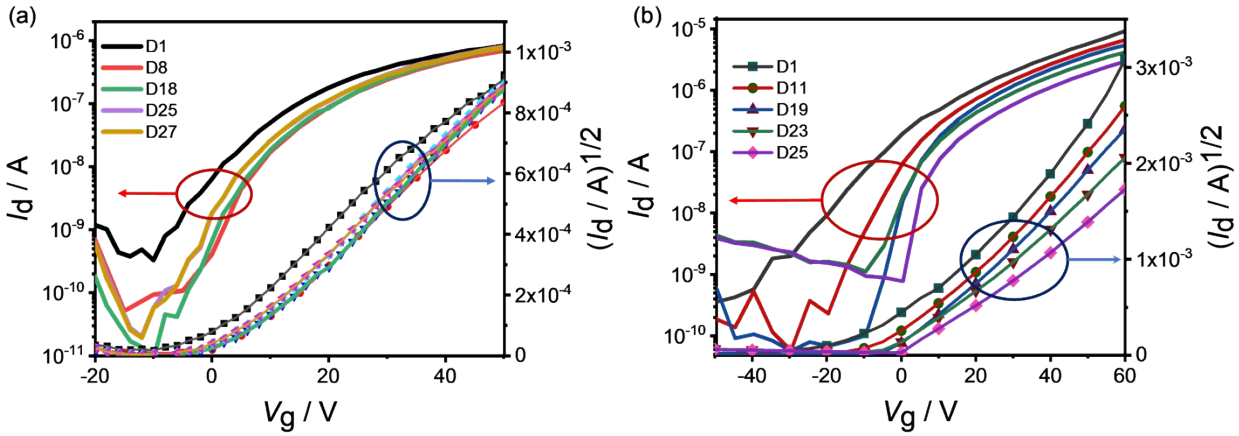


**Figure S11.** Transfer curves of the air-exposed devices at various intervals of time: a) **NDIFCN$_2$** and b) **EHNDICN$_2$**. (D = Day).

## 6. Single crystal structure:

Single crystals of **EHNDICN$_2$** were obtained from chloroform and *o*-dichlorobenzene solvent mixture by slow solvent evaporation and for **NDIFCN$_2$**, the solvent mixture was chloroform and ethyl acetate. **NDIFCN$_2$** recrystallizes in the monoclinic space group of $P2_1/c$ and **EHNDICN$_2$** as in the triclinic space group of $P\bar{1}$. A non-classical hydrogen bonding ($d_{C\text{-}H\cdots O}$ = 2.36 Å) and C-H interaction ($d_{C\text{-}H\cdots C}$ = 2.86 Å) are the major interactions that control the overall crystal packing of **EHNDICN$_2$**. There is slipped packing of the π-conjugated core with an inter-planar 3.34 Å π-stacking distance between two **EHNDICN$_2$** molecules. The low crystal packing density (1.3 g cm$^{-3}$) and the slipping angle along the long molecular axis is 67.09° and the short is 40.30° which indicates the low π–π overlapping between the molecules (figure S10c) and it reflects on the charge carrier mobility as low. In the case of **NDIFCN$_2$**, along with non-classical hydrogen bonding ($d_{C\text{-}H\cdots O}$ = 2.62 Å), H-F ($d_{C\text{-}H\cdots F}$ = 2.57, 2.61 Å) and F-F interactions ($d_{C\text{-}F\cdots F}$ = 2.85 Å) are the major interactions in the crystal packing (figure S11b). Including these interactions, strong C-F interactions ($d_{C\text{-}F\cdots C}$ = 2.90, 3.13 and 3.14 Å) help to pack with a high packing density (1.95 g cm$^{-3}$) in its crystal packing. Although having a high packing density, there is almost no direct π–π overlap between the two **NDIFCN$_2$** molecules. In figure S10b, it is visible that there is the incorporation of a fluro-alkyl chain through the π–π stacking direction. It prevents the π core-overlapping and

smooth charge transporting. As a result, we are observing even lower charge carrier mobility than **EHNDICN$_2$**.

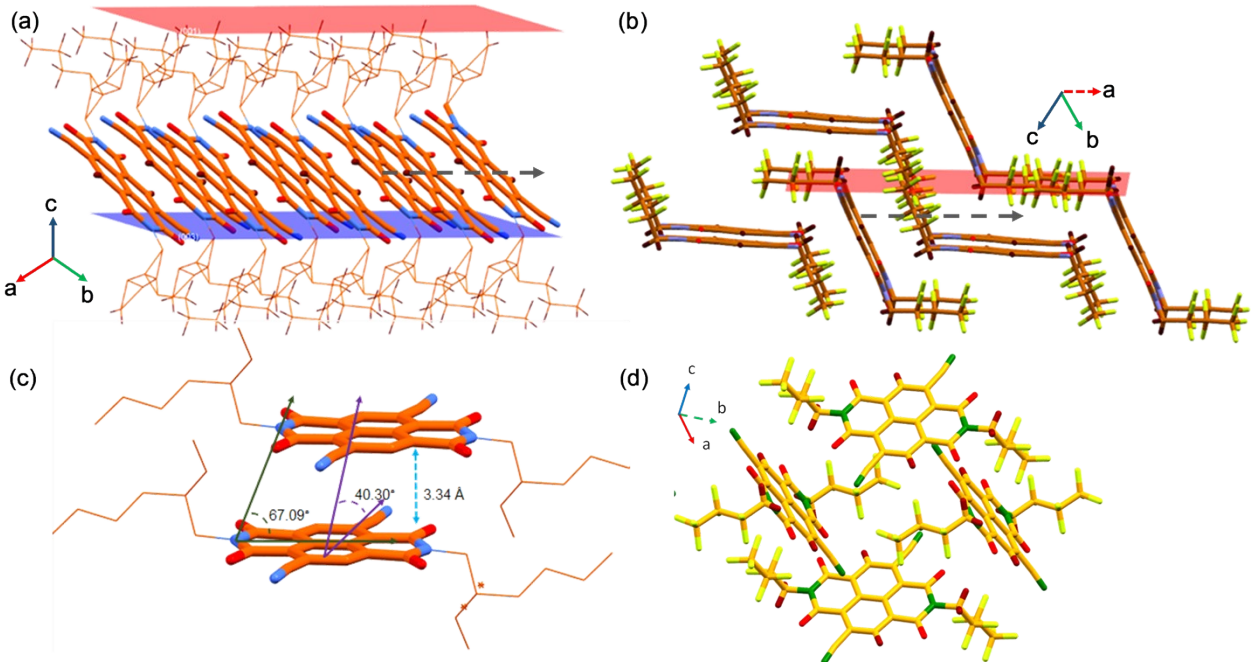


**Figure S12.** Single crystal structures with π stacking directions: (a), (c) for **EHNDICN$_2$** and (b), (d) for **NDIFCN$_2$** respectively (Black dotted arrow indicates charge transport direction).

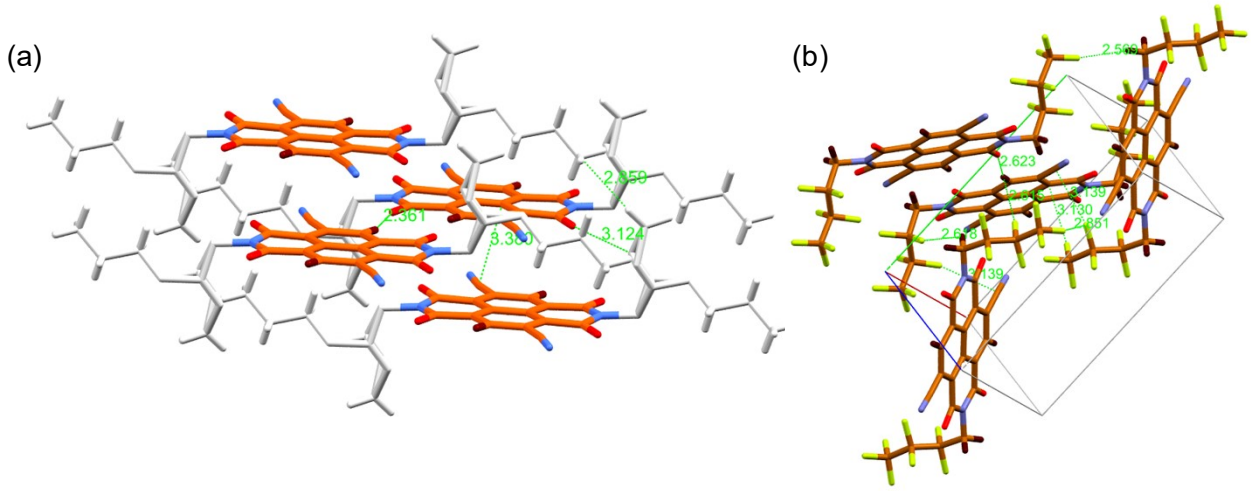


**Figure S13.** Major interactions in the crystal state packing: a) **EHNDICN$_2$** & b) **NDIFCN$_2$**.

**X-Ray Crystallographic Analysis:**

| | **$EHNDICN_2$** | **$NDIFCN_2$** |
|---|---|---|
| Chemical formula | C32 H34 N4 O4 | C24 H6 F14 N4 O4 |
| Crystal System | triclinic | monoclinic |
| Space Group | $P\bar{1}$ | P 1 21/c 1 |
| a (Å) | 5.3597 | 9.6378 |
| b (Å) | 8.2900 | 13.1727 |
| c (Å) | 15.7629 | 10.2479 |
| α (°) | 99.995 | 90 |
| β (°) | 93.825 | 117.064 |
| γ (°) | 95.201 | 90 |
| V ($Å^3$) | 684.48 | 1158.57 |
| Z | 1 | 4 |
| D (g $cm^{-3}$) | 1.307 | 1.950 |
| $R_1$ (%) | 9.67 | 3.39 |

**Table S1.** Crystallographic data obtained from single crystal XRD experiment.

**X-Ray Crystallographic interactions.**

| **$NDIFCN_2$** | **distance (Å)** | **$EHNDICN_2$** | **distance (Å)** |
|---|---|---|---|
| H9B-F13 | 2.569 | O001-C00K | 3.12 |
| F17-F14 | 2.85 | C00C-C006 | 3.38 |
| F17-C22 | 3.14 | N004-H4B | 2.58 |
| H3-O21 | 2.623 | N004-H00C | 2.74 |
| H3-F16 | 2.615 | H00B-O002 | 2.36 |
| C3-F16 | 2.896 | O001-H00Q | 2.35 |
| F18-H9A | 2.618 | | |
| C22-F17 | 3.14 | | |
| C5-F15 | 3.13 | | |

**Table S2.** Different types of non-classical interactions and their distances in their crystal state packing.

## 7. Film morphology analysis:

An atomic force microscopy experiment was carried out on NT-MDT (model no. AP-0100) in semi-contact mode. The morphology of the surfaces was investigated using field emission scanning electron microscopy (FE-SEM). The images were taken using an FE-SEM apparatus (ZEISS scanning microscope-ZSM-S 55 VP). The samples were prepared by keeping the conditions the same as device fabrication. For the spin-coated film, the roughness measured from AFM measurement is 2.4 and 2.8 nm, for **$NDIFCN_2$** and **$EHNDICN_2$** respectively. Low roughness indicates the smoothness of the films.

## 8. Film state-wide angle X-ray diffraction (WAXRD) and 2D grazing incident XRD (2D GIXRD):

Film state-wide angle X-ray diffraction (WAXRD) measurements were conducted for **$EHNDICN_2$** on OTS-modified $SiO_2$ and **$NDIFCN_2$** on bare $SiO_2$ substrates. A solution of **$EHNDICN_2$** was prepared in Chloroform (5 g $L^{-1}$) at 45 °C and **$NDIFCN_2$**, a solution of 4-5 g $L^{-1}$ in o-dichlorobenzene (*o*-DCB) was prepared at 120 °C and stirring condition. For **$NDIFCN_2$**, the film was made by drop casting and for **$EHNDICN_2$**, the film was made by spin coating with 1500 rpm spin speed for 40 s. The substrates were further subjected to thermal annealing at 120 °C for 10 minutes and then transferred to a vacuum desiccator. For 2D XRD measurements, samples were prepared on top of glass substrate keeping the device fabrication conditions same.

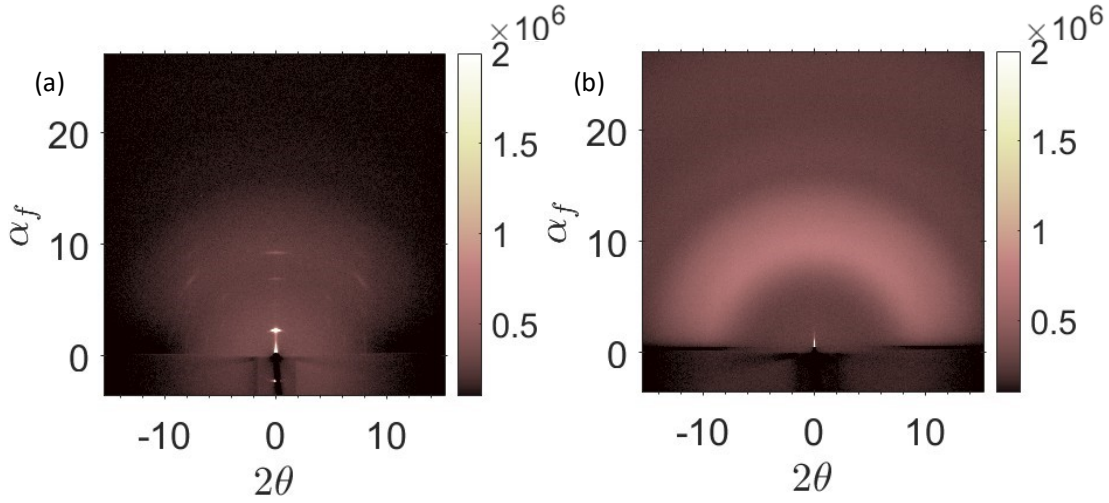


**Figure S14.** 2D GIXRD pattern (a) **EHNDICN2,** (b) **$NDIFCN_2$**.

## 9. Contact angle measurement:

For water contact angle measurement, we made the film on top of $Si/SiO_2$ substrates keeping all the conditions the same as device fabrications. The greater contact angle of **$NDIFCN_2$** (108 º) than **$EHNDICN_2$** (94 º) indicates the higher hydrophobicity in the case of the fluorinated alkyl chain containing **NDI**. As a result, we observed the higher ambient stable device in the case of **$NDIFCN_2$**. Contact angle measurements were repeated, with the same drops left on the substrates for a duration. Results showed that for **$NDIFCN_2$**, there was scarcely any change in the contact angle even after 150 seconds, with a marginal decrease from 108 ° to 105 °. Conversely, **$EHNDICN_2$** exhibited a significant alteration in contact angle after just 50 seconds, decreasing from 94 ° to 75 °. These findings indicate the superior hydrophobicity of **$NDIFCN_2$** compared to **$EHNDICN_2$**. Live video was also added.

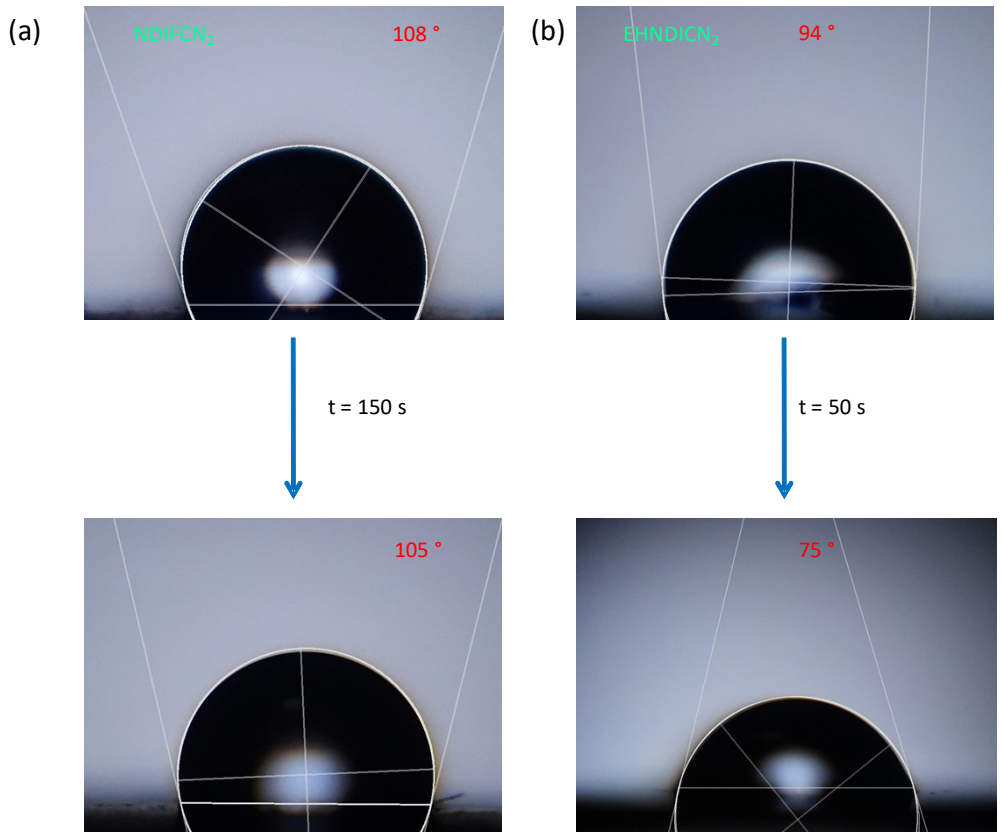


**Figure S15.** The contact angle of a water droplet on the thin films of a) **$NDIFCN_2$** and b) **$EHNDICN_2$**, over a period of seconds.

## 10. FTIR Spectroscopy Measurements:

For FTIR spectroscopy, the compound was drop-casted from a chloroform solution onto an IR fused quartz substrate. Subsequently, it was annealed at 120 °C for 10 minutes and then placed in a vacuum desiccator overnight. Measurements were conducted on day 1, day 7, and day 30.

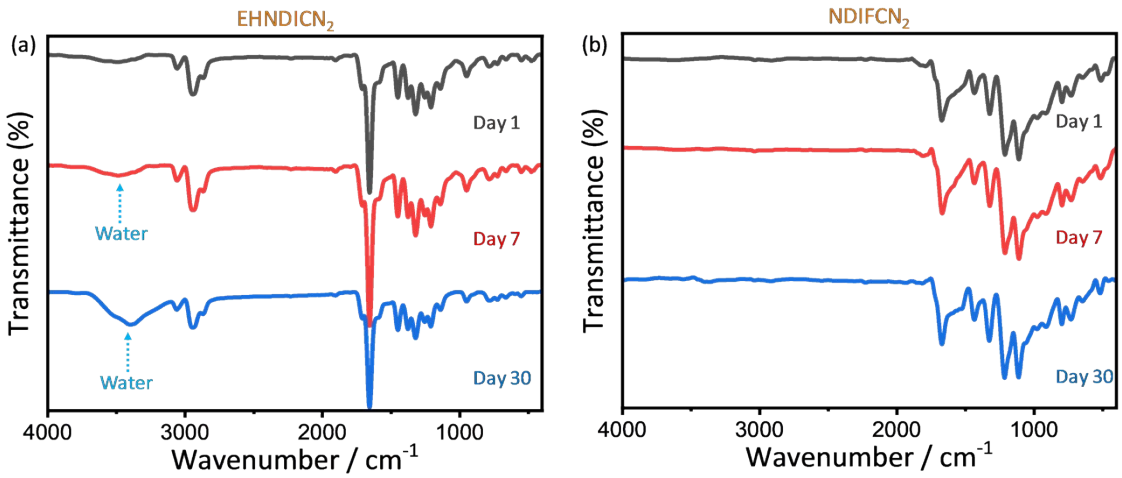


**Figure S16.** FTIR spectroscopy of (a) $EHNDICN_2$ and (b) $NDIFCN_2$ films exposed to ambient atmosphere for 30 days.

## 11. References:


1 B. A. Jones, A. Facchetti, T. J. Marks and M. R. Wasielewski, *Chem. Mater.*, 2007, **19**, 2703–2705.